Fractional Order Processing of Satellite Images

Manuel Henriques[1,†]

Abstract—Nowadays, satellite images are used in many applications, and their automatic processing is vital. One objective of this investigation was to evaluate the use of fractional derivatives on edge detection in the aforementioned scope. The state of the art on this matter concludes that the fractional methods enhance the results of contour detection and improve immunity to noise in image processing. It also states that color-based processing can achieve better results. However, in the already existent applications there is a difficulty in achieving fixed parameters that optimize the performance in edge detection. This study shows that using fractional derivatives in edge detection methods, for both grey-scale and colour Sentinel-2 images, may enhance the results obtained using conventional techniques. It also finds a fixed set of parameters that allow automatic detection maintaining high performance.

Index Terms—Satellite, Fractional Derivative, Automatic Detection, Color-Based Detection, Grey-Scale Detection, Fractional Processing

1 Introduction

IMAGE processing has always been an essential tool in remote sensing. The processing of images taken by satellites may be used in many areas such as land monitoring, routine mapping and surveillance [1].

Edge detection represents an important role in remote sensing. Conventional edge detectors are based on integer derivatives. With the introduction of fractional calculus, some new non-integer edge detectors were created [2] and the existent integer ones adapted [3], [4], [5].

The aforementioned detectors were developed for grey scale images. Since the input is often a colored image, it must be converted. This may compromise the performance of edge detection. Thus, color-based edge detection detectors were created. [6], [7].

One goal of this paper is to apply fractional edge detection to satellite images. For this, an algorithm that receives satellite images of coasts and performs edge detection in order to differentiate land from water was implemented. Three types of detectors were analysed: conventional grey-scale integer detectors, grey-scale fractional and color-based fractional ones. The former two can be found in the literature; to the best of our knowledge, colour-based fractional detectors presented in this paper are the first ever used with the exception of Canny already given in [6].

Other objective is to assess if it is possible to implement an automatic solution with fixed parameters that allows automatic detection of coasts. Experiences with medical images suggest that this may be unclear [8], [9].

This paper is organised as follows: Section 2 explains the theoretical formulations for the edge detectors tested, Section 3 explains the proposed implementation and the performance metrics, in Section 4 the experimental results are presented and in Section 5 the conclusions are drawn.

[1] *Departamento de Engenharia Mecânica, Instituto Superior Técnico, Universidade de Lisboa; manuel.henriques@tecnico.ulisboa.pt*
[†] *Current address: Av. Rovisco Pais 1, 1049-001 Lisboa, Portugal*

2 Definitions and Formulations

In this section, the main definitions and different formulations relevant to the study will be presented.

2.1 Grünwald-Letnikov (GL) Definition

The truncated GL definition of fractional derivative used in formulations for fractional detectors in this study is: .

$$ {}_cD_t^{\alpha} f(t) = \lim_{h\to 0} h^{-\alpha} \sum_{k=0}^{N} (-1)^k \binom{\alpha}{k} f(t-kh), N = \left\lceil \frac{t-c}{h} \right\rceil, \quad t > c \tag{1} $$

where combinations of a things, b at a time, are generalised using the Gamma function as [10]:

$$ \binom{a}{b} = \begin{cases} \frac{\Gamma(a+1)}{\Gamma(b+1)\Gamma(a-b+1)}, & \text{if a, b, a-b} \notin Z^- \\ \frac{(-1)^b \Gamma(b-a)}{\Gamma(b+1)\Gamma(-a)}, & \text{if } a \in Z^- \wedge b \in Z_0^+ \\ 0, \text{ if } \left[\left(b \in Z^- \vee b-a \in N\right) \wedge a \notin Z^-\right] \vee \\ \quad \left(a, b \in Z^- \wedge |a| > |b|\right) \end{cases} \tag{2} $$

2.2 Canny Edge Detector

Original BW: The Canny edge detector is a popular edge detection algorithm [11]. The image is first convolved with a Gaussian Filter and then, a first derivative operator is applied to the smoothed image in order to compute gradients (in this study the derivative of the smoothing Gaussian function was used).

Fractional BW: The fractional version of this operator may be implemented by switching the integer operator with a fractional order derivative one using GL definition. The remaining steps of the algorithm remain unchanged.

Colour: Kanade introduced a color-based version of the operator [6]. It is based on the same steps as the conventional Canny but the computations are vector based. This means that the algorithm determines the first partial derivatives of the smoothed image in both x and y directions for each color channel which define the following Jacobian:

$$\mathbf{J} = \begin{pmatrix} R_x & R_y \\ G_x & G_y \\ B_x & B_y \end{pmatrix} = (\mathrm{C}_x, \mathrm{C}_y) \tag{3}$$

The direction in the image along which the largest variation in the chromatic image function occurs is represented by the eigenvector of $J^T J$ corresponding to the largest eigenvalue.

$$\mathbf{J^T J} = \begin{pmatrix} J_x & J_{xy} \\ J_{yx} & J_y \end{pmatrix} \tag{4}$$

$$\lambda = \frac{J_y + J_x \pm \sqrt{(J_y + J_x)^2 - 4(J_x J_y - J_{xy}^2)}}{2} \tag{5}$$

According to experiments in Carnegie Mellon University [12], the color edges describe object geometry in the scene better than the intensity edges, although over 90% of the edges are identical.

2.3 Sobel Edge Detector

Original BW: The integer Sobel operator performs a derivative operation on an image and so it highlights regions where there are sudden increases of pixel intensity which correspond to edges. The operator consists of two masks (6).

-1	0	$+1$
-2	0	$+2$
-1	0	$+1$

$+1$	$+2$	$+1$
0	0	0
-1	-2	-1

(6)

The resulting image gradient components can be expressed as:

$$\begin{aligned} G_x = &-f(x-1,y-1) - 2f(x-1,y) - f(x-1,y+1) \\ &+ f(x+1,y-1) + 2f(x+1,y) + f(x+1,y+1) \end{aligned} \tag{7}$$

Fractional BW: By applying the G-L definition (1) to G_x expressed in (7), the fractional derivative can be obtained by convolving the image $f(x, y)$ with the filter mask presented in (8):

$\frac{\alpha(-\alpha+1)(-\alpha+2)}{12}$	$\frac{\alpha(-\alpha+1)(-\alpha+2)}{6}$	$\frac{\alpha(-\alpha+1)(-\alpha+2)}{12}$
$\frac{\alpha(-\alpha+1)}{4}$	$\frac{\alpha(-\alpha+1)}{2}$	$\frac{\alpha(-\alpha+1)}{4}$
$\frac{\alpha}{2} - \frac{\alpha(-\alpha+1)(-\alpha+2)}{12}$	$\alpha - \frac{\alpha(-\alpha+1)(-\alpha+2)}{6}$	$\frac{\alpha}{2} - \frac{\alpha(-\alpha+1)(-\alpha+2)}{12}$
$-\frac{1}{2} - \frac{\alpha(-\alpha+1)}{4}$	$-1 - \frac{\alpha(-\alpha+1)}{2}$	$-\frac{1}{2} - \frac{\alpha(-\alpha+1)}{4}$
$-\frac{\alpha}{2}$	$-\alpha$	$\frac{\alpha}{2}$
$\frac{1}{2}$	1	$\frac{1}{2}$

(8)

According to the authors, the proposed edge detector was able to reduce the number of false edge pixels while presenting thinner edges, compared to the conventional Sobel-based edge detector.

Colour: A novel color-based fractional Sobel was implemented by applying the same color-based formulation of section 2.2 with the mask in (8).

2.4 Roberts Edge Detector

Original BW: The integer Roberts operator [13] consists of a pair of 2x2 masks:

$+1$	0
0	-1

0	$+1$
-1	0

(9)

Fractional BW: In [4], a fractional Roberts detector is presented. Based on the truncated coefficients of the GL definition, the authors of this work constructed an operator that applies derivatives of arbitrary order α (10).

$\frac{\alpha^2-\alpha+2}{2}$	$\frac{\alpha^2-\alpha+2}{2}$	$\frac{\alpha^2-\alpha+2}{2}$
$\frac{\alpha^2-\alpha+2}{2}$	-8α	$\frac{\alpha^2-\alpha+2}{2}$
$\frac{\alpha^2-\alpha+2}{2}$	$\frac{\alpha^2-\alpha+2}{2}$	$\frac{\alpha^2-\alpha+2}{2}$

(10)

This mask is applied after the convolution of an image with the conventional integer Sobel. From the experimental results in [4], it was concluded that the improved algorithm has the advantages of Roberts, that is, obtaining thinner edges, besides allowing edge enhancement.

Colour: The reasoning used to implement the color-based Sobel operator was also used here. The fractional operator requires convolutions with two masks. The color-based vector convolution and computations were applied only to the first one with the integer Roberts. Then, the output of this first integer color-based edge detection is the input to the fractional derivative operation.

2.5 Laplacian of Gaussian Detector

Original BW: In image processing, the Laplacian is a measure of the 2^{nd} spatial derivative of an image. Three possible Laplacian operators are:

0	1	0
1	-4	1
0	1	0

1	1	1
1	-8	1
1	1	1

-1	2	-1
2	-4	2
-1	2	-1

(11)

To tackle sensitivity of second order derivatives to noise, the image is Gaussian smoothed before applying the Laplacian filter reducing high frequency noise. The smoothing filter can also be convolved first with the Laplacian kernel and only then is the result convolved with the input image.

Fractional BW: In 2014, the authors of [5] presented a fractional adaptation for the first operator in (11) (using the symmetric mask) and the GL definition .

0	$\dots$	0	$(-1)^{\kappa} C_{K-1}^{\alpha}$	0
$\vdots$	$\vdots$	$\vdots$	$\vdots$	$\vdots$
0	$\dots$	0	$\left(\alpha - \alpha^2\right)/2$	0
$(-1)^{\kappa} C_{K-1}^{\alpha}$	$\dots$	$\left(\alpha - \alpha^2\right)/2$	2α	-1
0	$\dots$	0	-1	0

(12)

Colour: A novel color-based fractional LoG operator was implemented and tested in this study. The conventional algorithm finds edges searching for zero-crossings. This means that previous formulations cannot be adapted. According to [14], a pixel of a color image is considered as part of an edge if zero-crossings are found in any of the color channels. An algorithm that convolves the fractional LoG mask with the different color channels of an input image was implemented. The algorithm then searches for zero-crossings in each of the convolution outputs and, if a

zero-crossing is found, the corresponding pixel is flagged as one. The output of the algorithm is a binary image with all edges found.

2.6 CRONE

In 2002, Benoît Mathieu wanted to prove that an edge detector based on fractional differentiation could improve edge detection and detection selectivity in the case of parabolic luminance transition. Thus and using GL definition he developed the CRONE operator [2]:

$$\underset{\leftrightarrow}{D}^{n} f(x) = \frac{1}{h^n} \sum_{k=0}^{\infty} a_k [f(x - kh) - f(x + kh)] \tag{13}$$

$$\begin{aligned} a_k &= (-1)^k \begin{pmatrix} n \\ k \end{pmatrix} \\ &= (-1)^k \frac{n(n-1)\cdots(n-k+1)}{k!} \end{aligned} \tag{14}$$

In order to detect edges on images, the formulated detector can be used in 2D with mask (15) and its transposed:

$$\begin{bmatrix} +a_m & \cdots & +a_1 & 0 & -a_1 & \cdots & a_m \end{bmatrix} \tag{15}$$

In this paper, a novel color-based fractional CRONE is implemented following the same steps as in the color Canny already formulated.

2.7 Fractional Derivative Operator

The fractional mask used in the fractional Roberts is used in addition to the conventional integer mask. In this study the Fractional Derivatives mask in (10) was implemented individually as a fractional edge detector.

A new color-based version for this detector was also implemented. In this case there is only one mask to detect edges in eight different directions. Thus, the Jacobian is reduced to a vector (one dimension).

3 Implementation

All edge detectors were implemented in MATLAB to perform fractional detection. In this study, forty-three random images with low nebulosity from ESA's Sentinel-2 satellite [15] were used. The images retrieved from the website were analysed and a ground truth was manually taken using GIMP.

3.1 Main Algorithm Description

To process images, a main script was developed where the different edge detectors were introduced. This algorithm included the loading of images and ground truths, pre and post-processing (including a blue color filter in order to avoid noise in the water and morphological operations to close land contours), the *edge* detection function and performance analysis.

TABLE 1
Performance Instances.

		Processed Image	
		0	1
Ground Truth	0	TN	FP
	1	FN	TP

3.2 Performance Assessment

In order to check performance, quantification has to be made. For that, the ground truth is compared to the output of the algorithm by scanning all pixels within the image. Four instances may occur: True Positives, False Positives, True Negatives and False Negatives (Table 1).

Using the number of occurrences of each instance the following metrics were computed:

$$J(A, B) = \frac{TP}{FP + TP + FN} \tag{16}$$

$$DSC = \frac{2 \times TP}{2 \times TP + FP + FN} \tag{17}$$

$$\text{Sensitivity} = \frac{TP}{TP + FN} \tag{18}$$

$$\text{Specificity} = \frac{TN}{FP + TN} \tag{19}$$

During the study it was concluded that the Jaccard coefficient (J) is a good overall performance metric since the results with the highest J corresponded to the ones with maximum mean performance regarding the four metrics. Thus, the Jaccard coefficient is used as overall performance indicator.

4 Results

The formulated detectors were implemented modifying the custom *edge* function and tested for a set of parameters. In this section, the overall relevant results of the iterations with different parameters will be presented. The total extended results are available in Excel files from a public Google Drive [16].

4.1 Performance Analysis of Fractional vs Integer Edge Detection

The first step of performance analysis is to understand in each edge detection algorithm, if a fractional order based adaptation thereof outperforms the conventional integer version. Therefore, all the algorithms formulated in chapter 2 were tested for a set of parameters and the results will be presented. The performance was evaluated for all 43 images in the database using the metrics introduced in section 3.2. From the forty three figures, four were chosen to carry out individual performance assessment in this section. For space reasons, in this document results for only one image will be presented. The selected figure was number 38 presented with its corresponding ground truth in Figure 1.

The best performances of the different detectors for image 38 are presented in Figure 2 and Table 2.

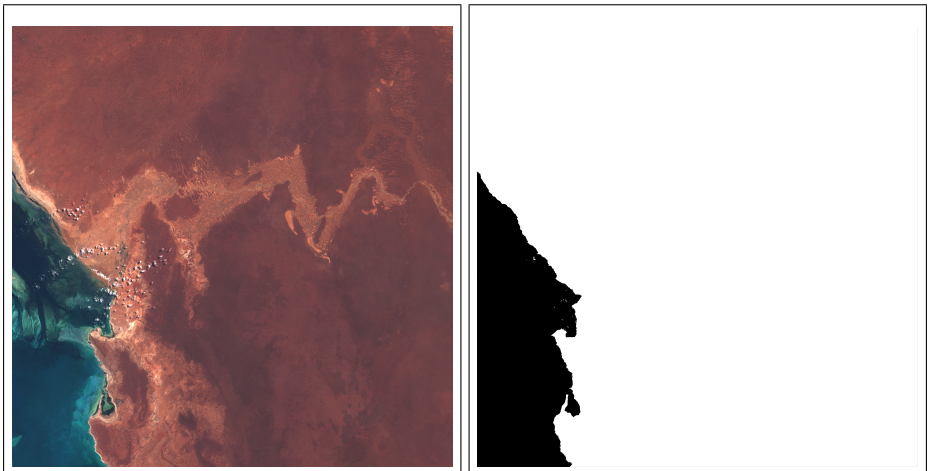

(a) Coast_D(38) (b) Ground Truth

Fig. 1. Figure number 38 to be evaluated with corresponding ground truth.

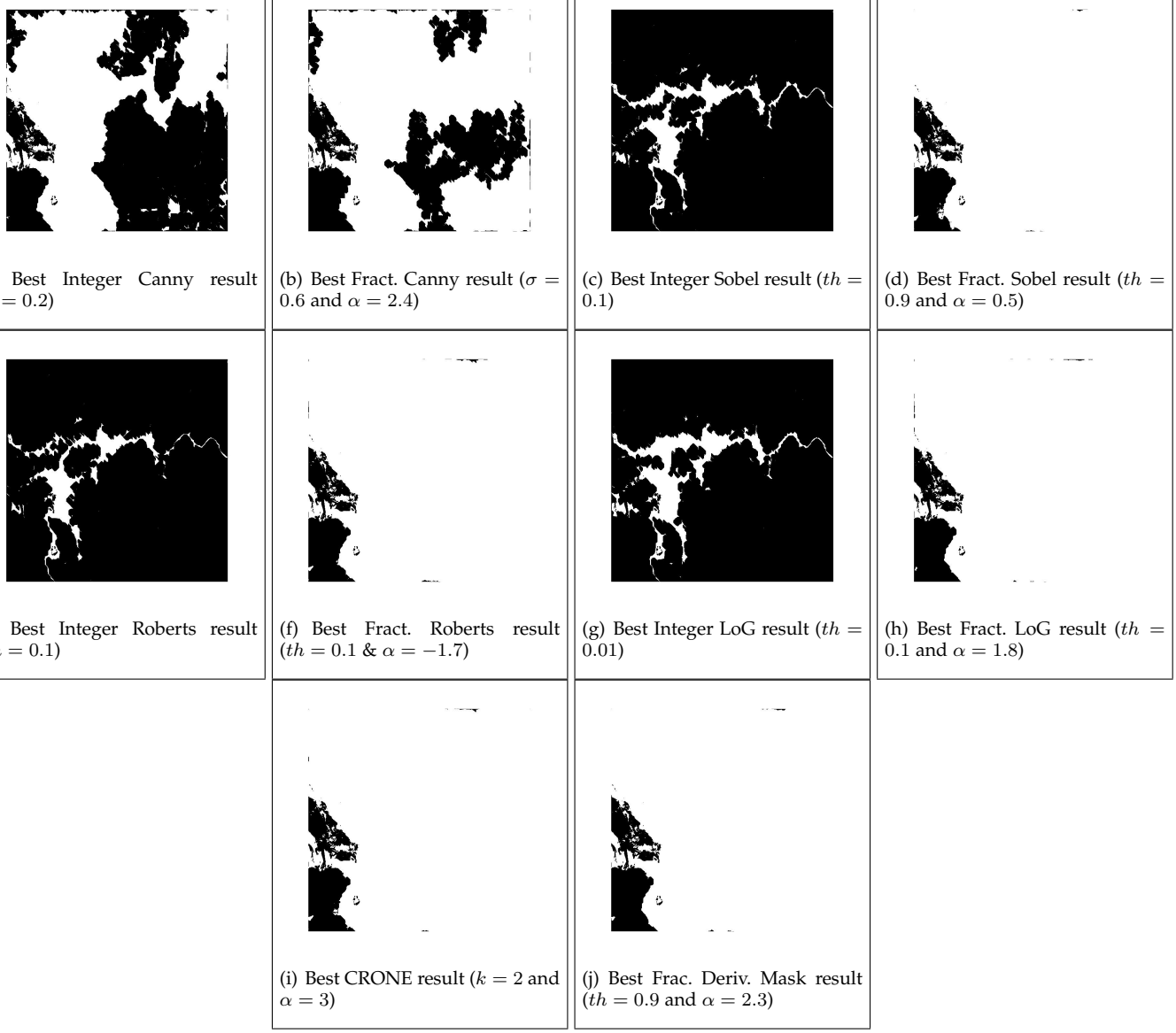

(a) Best Integer Canny result ($\sigma = 0.2$)

(b) Best Fract. Canny result ($\sigma = 0.6$ and $\alpha = 2.4$)

(c) Best Integer Sobel result ($th = 0.1$)

(d) Best Fract. Sobel result ($th = 0.9$ and $\alpha = 0.5$)

(e) Best Integer Roberts result ($th = 0.1$)

(f) Best Fract. Roberts result ($th = 0.1$ & $\alpha = -1.7$)

(g) Best Integer LoG result ($th = 0.01$)

(h) Best Fract. LoG result ($th = 0.1$ and $\alpha = 1.8$)

(i) Best CRONE result ($k = 2$ and $\alpha = 3$)

(j) Best Frac. Deriv. Mask result ($th = 0.9$ and $\alpha = 2.3$)

Fig. 2. Best results for Figure 38 processed using Fractional and Integer algorithms.

TABLE 2
Table with best performance results using Grey-Scale edge detectors on image 38

Method	k	σ	threshold	α	J	D	Sensitivity	Specificity
Integer Canny	-	0.2	-	-	0.5180	0.6825	0.5365	0.7167
Fractional Canny	-	0.6	-	2.4	0.7356	0.8477	0.7600	0.7359
Integer Sobel	-	-	0.1	-	0.0768	0.1427	0.0775	0.9271
Fractional Sobel	-	-	0.9	0.5	0.9600	0.9796	0.9997	0.6710
Integer Roberts	-	-	0.1	-	0.0618	0.1163	0.0622	0.9451
Fractional Roberts	-	-	0.1	-1.7	0.9613	0.9803	0.9990	0.6877
Integer LoG	-	-	0.01	-	0.0887	0.1630	0.0898	0.9076
Fractional LoG	-	-	0.1	1.8	0.9637	0.9815	0.9994	0.7046
CRONE	2	-	-	3	0.9612	0.9802	0.9995	0.6818
Fract. Deriv. Mask	-	-	0.9	2.3	0.9625	0.9809	0.9995	0.6936

4.2 Grey-Scale Edge Detectors vs Color Based Edge Detectors

As explained before, color edge detection algorithms were also implemented and tested to the whole data set due to their good results in other applications. All the six methods were adapted and applied in the main algorithm in order to perform color-based edge detection. The best results of the performance assessment for this versions of the algorithms are presented above and are compared with the corresponding best grey-scale result. This comparison is presented under the form of histograms for each detector in Figure 3. Due to scale issues, the y-axis values which corresponded to ΔJ were transformed to $10^{\Delta J}$.

4.3 Overall Performance with Varying Parameters

To analyse the overall performance of detectors, the mean Jaccard of the best results for each edge detection operator (for all images in the data set) was computed. The results are shown in Table 3 .

TABLE 3
Ranking of the best results average for all images.

Detector	$\overline{J}$
Fractional Derivative Op.	0.9623
Color Fractional Derivative Op.	0.9596
Color Laplacian of Gaussian	0.9554
Color Roberts	0.9537
Laplacian of Gaussian	0.9531
Color Sobel	0.9478
Roberts	0.9474
Color CRONE	0.9461
Color Canny	0.9448
CRONE	0.9447
Canny	0.9342
Sobel	0.9282

4.4 Overall Performance with Fixed Parameters

One crucial objective of this work is to access if it is possible to find and easily tune parameters, in an automatic way without loosing performance. Thus, in this section, the results of the search for optimal fixed parameters will be presented. Hence, the performance results were sorted to find the best results using fixed parameters for all the images in the data set. Table 4 presents the best fixed parameters results for each detector.

The performance with fixed parameters was also analysed by plotting the mean performance (for all images) across the range of parameters. This is illustrated in the plots of Figures 4 and 5. As one may observe, the surface plots are well defined and present generally smooth evolution. This contrasts with investigations regarding medical images [8], [9] and allows the optimization of parameters for an automatic solution.

TABLE 4
Best results with fixed parameters for all detectors (Whole Data Set).

Detector	$threshold$	k	σ	α	$\overline{J}$
Color Fractional Derivative Op.	0.9	-	-	0.8	0.9436
Fractional Derivative Op.	0.7	-	-	0.8	0.9428
Color CRONE	-	5	-	0.9	0.9328
CRONE	-	5	-	1.1	0.9261
Color Canny	-	-	0.7	1.7	0.9193
Color Roberts	0.1	-	-	1.4	0.9174
Color Sobel	0.3	-	-	-0.2	0.9153
Sobel	0.9	-	-	0.2	0.9111
Color Laplacian of Gaussian	0.1	-	-	-0.9	0.9108
Roberts	0.1	-	-	-1.3	0.9076
Laplacian of Gaussian	0.1	-	-	-1.4	0.9028
Canny	-	-	0.6	0	0.9011

5 Conclusion

In this paper, an automatic coasts edge detection tool using five state-of-the-art edge detection versions and seven novel detector versions was presented. The conventional integer versions of the algorithms were also tested and compared to fractional solutions.

Forty-three high definition (10980p×10980p) satellite images were tested using the different versions of the operators in a wide range of parameters.

The data presented in Section 4.1, together with the performance of other images available in [16], allows to conclude that the use of fractional derivatives in edge detection for this application matched or improved, in most cases, the performance of the conventional integer methods.

The color based algorithms allowed to equal or improve the performance of grey-scale methods in most cases. However, often the increase in performance is low in percentage.

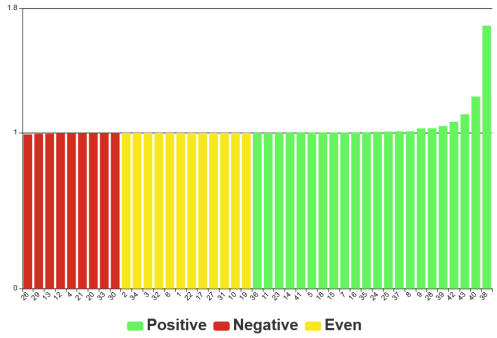

(a) Canny

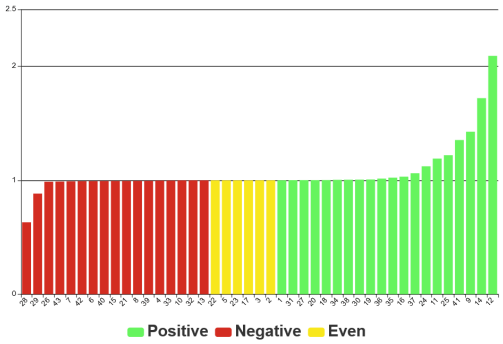

(b) Sobel

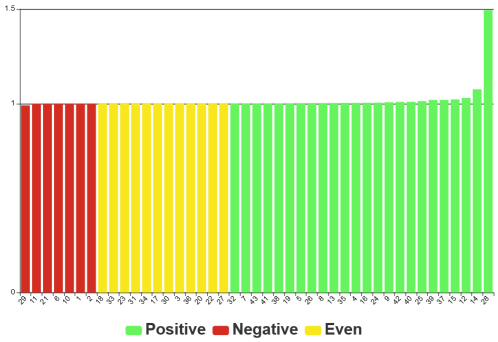

(c) Roberts

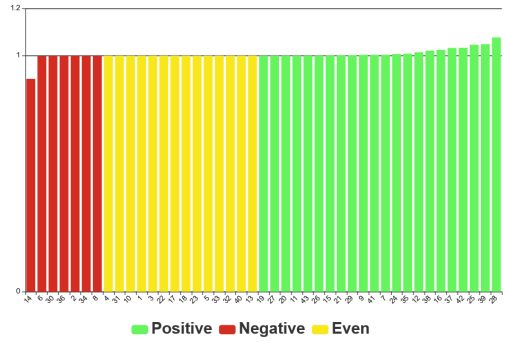

(d) LoG

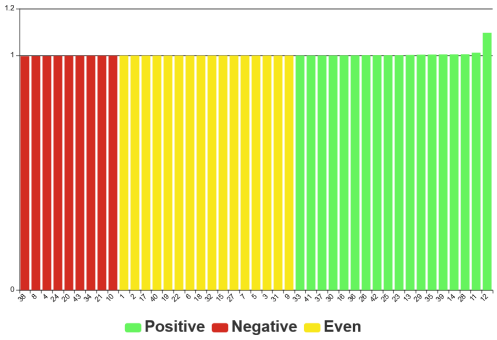

(e) CRONE

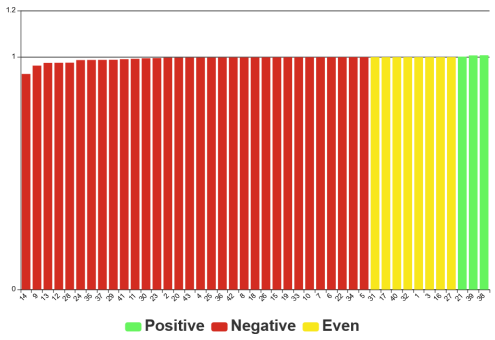

(f) Fract. Deriv. Mask

Fig. 3. Analysis of performance comparison between grey-scale and color based detectors (Exponential Version).

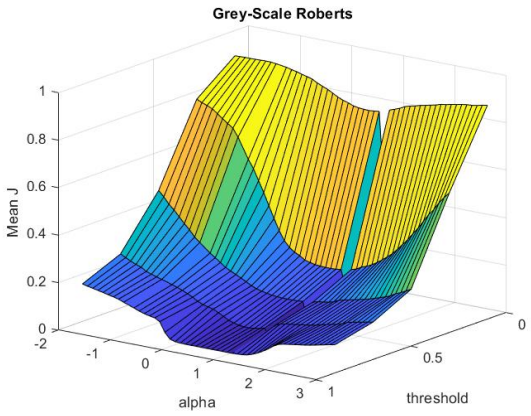

(a) Grey-Scale Roberts

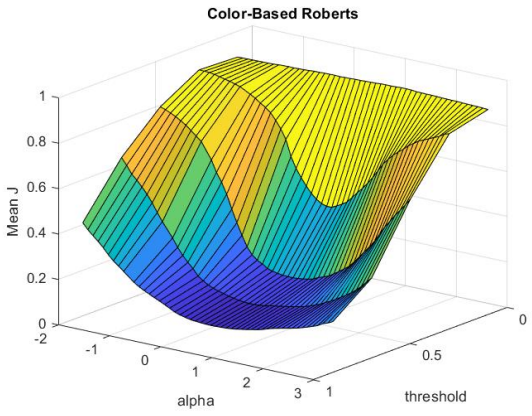

(b) Color-Based Roberts

Fig. 4. Mean Performance of Roberts algorithms graphs using same parameters for all images.

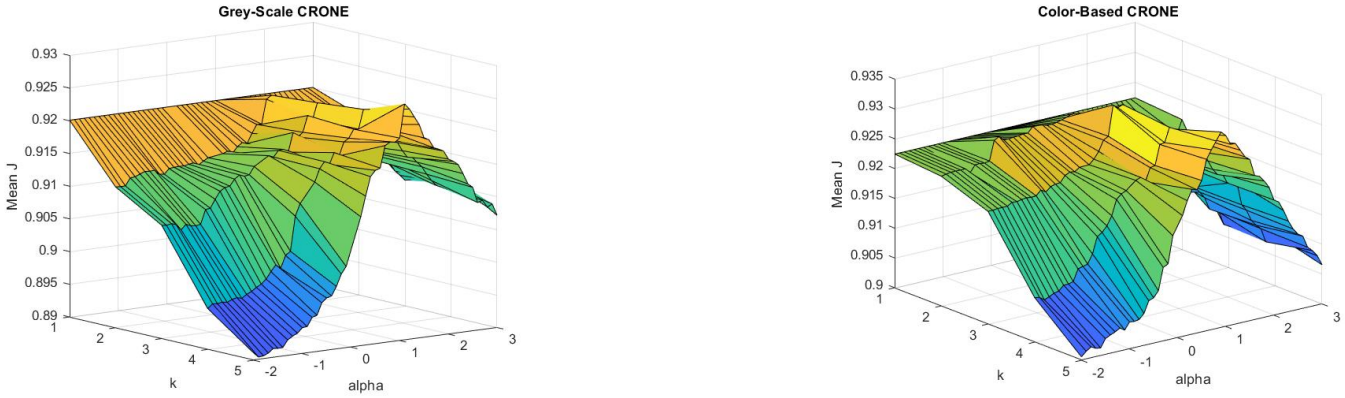

(a) Grey-Scale CRONE (b) Color-Based CRONE

Fig. 5. Mean Performance of CRONE algorithms graphs using same parameters for all images.

Nevertheless, and since we are dealing with images that are composed of more than 120 million pixels, a percentage of 1% increase corresponds to more than 1 million pixels correctly identified. The color based detector is also heavier computationally since it usually requires more than one convolution (at least one for each color channel). The use of this type of operators in the context of this thesis may be useful if one is not satisfied with the results of grey-scale identification.

The grey scale Fractional Derivatives operator was the detector that provided the best average scores regarding all figures, with varying parameters. The mean Jaccard coefficient for this operator was 0.9623. This means that the algorithm identified correctly in average 96.23% of the pixels in the input images.

In remote sensing, it is important not only that the algorithm can reach high efficiency but also that the parameters required are possible to implement for an automatic solution. Despite the exceptional performance achieved with varying parameters, this Jaccard coefficient is only possible using a great spread of parameters impossible to reach in automatic solutions. Thus, the search for a solution with fixed parameters was conducted. In this case, the color-based Fractional Derivatives operator was the method that provided the best average scores regarding all figures in the data set, with a Jaccard metric of 0.9436. The result obtained constitutes a fixed-parameter solution that allows automatic detection of coasts with a decrease in performance compared to the aforementioned varying-parameters of less than 2%.

Further analysing overall performance tables 3 and 4 the extended results in the public drive [16], one may draw a few more conclusions. The usage of fractional derivatives in edge detection for this application matched or improved, in most cases, the performance of the conventional integer methods. The color based algorithms allowed to equal or improve the performance of grey-scale methods in most cases. However, often the increase in performance is low in percentage. Nevertheless, and since we are dealing with images that are composed of more than 120 million pixels, a percentage of 1% increase corresponds to more than 1 million pixels correctly identified.

To summarize, in this study it was developed a successful automatic tool that identifies and segments coasts in satellite images using both grey-scale and novel color-based fractional edge detectors and the subsequent parameters that allow the automation of the solution.

REFERENCES

[1] ESA, "Sentinel-2," https://sentinel.esa.int/web/sentinel/missions/\\sentinel-2/mission-objectives, 2020, (Visited on 12/06/2020).

[2] B. Mathieu, P. Melchior, A. Oustaloup, and C. Ceyral, "Fractional differentiation for edge detection," *Signal Processing*, vol. 83, no. 11, pp. 2421–2432, 2003.

[3] C. Yaacoub and R. A. Zeid Daou, "Fractional order sobel edge detector," in *2019 Ninth International Conference on Image Processing Theory, Tools and Applications (IPTA)*, 2019, pp. 1–5.

[4] X. Chen and X. Fei, "Improving edge-detection algorithm based on fractional differential approach," in *IPCSIT*, vol. 50, 2012.

[5] D. Tian, J. Wu, and Y. Yang, "A fractional-order laplacian operator for image edge detection," *Applied Mechanics and Materials*, vol. 536-537, pp. 55–58, 04 2014.

[6] T. Kanade and S. Shafer, "Image Understanding Research at Carnegie Mellon," in *Proceedings of a Workshop on Image Understanding Workshop*. San Francisco, CA, USA: Morgan Kaufmann Publishers Inc., 1989, p. 32–48.

[7] A. Cumani, "Edge detection in multispectral images," *CVGIP: Graphical Models and Image Processing*, vol. 53, no. 1, pp. 40–51, 1991.

[8] T. Bento, D. Valério, P. Teodoro, and J. Martins, "Fractional order image processing of medical images," *Journal of Applied Nonlinear Dynamics*, vol. 6, pp. 181–191, 06 2017.

[9] J. F. M. Gonçalves., "3d fractional order image processing for cancer detection," Master's thesis, Instituto Superior Técnico, 2018.

[10] D. Valério and J. S. da Costa, "Introduction to single-input, single-output fractional control," *IET Control Theory and Applications Vol. 5, no. 8*, p. 1033–1057, May 2011.

[11] J. Canny, "A computational approach to edge detection," *IEEE Transactions on pattern analysis and machine intelligence*, no. 6, pp. 679–698, 1986.

[12] A. Koschan and M. Abidi, "Detection and classification of edges in color images," *IEEE Signal Processing Magazine*, vol. 22, no. 1, pp. 64–73, February 2005.

[13] L. Roberts, "Machine perception of 3-d solids," Ph.D. dissertation, Massachusetts Institute of Technology, 1963.

[14] S.-Y. Zhu, K. N. Plataniotis, and A. N. Venetsanopoulos, "Comprehensive analysis of edge detection in color image processing," *Optical Engineering*, vol. 38, no. 4, pp. 612–625, April 1999.

[15] ESA, "Copernicus open access hub," https://scihub.copernicus.eu/, 2020, (Visited on 31/03/2020).

[16] M. Henriques, "Results Repository," https://drive.google.com/drive/folders/1GMeKvc3oqNWfzd4h-GyRwHT9yFJ_UDLP?usp=sharing.